THE EFFECTIVENESS OF USING VISCOELASTIC MATERIALS TO REDUCE SEISMIC INDUCED VIBRATIONS OF ABOVE GROUND PIPELINES

Kaming Bi[1,*] and Hong Hao[1]
[1] Centre for Infrastructure Monitoring and Protection (CIMP),
School of Civil and Mechanical Engineering, Curtin University,
Kent Street, Bentley WA 6102, Australia.*Email:kaiming.bi@curtin.edu.au

ABSTRACT

Pipeline systems are commonly used to transport oil, natural gas, water, sewage and other materials. They are normally regarded as important lifeline structures. Ensuring the safety of these pipeline systems is crucial to the economy and environment. There are many reasons that may result in the damages to pipelines and these damages are often associated with pipeline vibrations. Therefore it is important to control pipeline vibrations to reduce the possibility of catastrophic damages. This paper carries out numerical investigations on the effectiveness of using viscoelastic material layers to mitigate seismic induced vibrations of above ground pipelines. The numerical analyses are carried out by using the commercial finite element code ANSYS. The numerical model of the viscoelastic material is firstly calibrated based on the experimental data obtained from a 1.6m long tubular sandwich structure. The calibrated material model is then applied to the pipeline system. The effectiveness of using viscoelastic materials as the seismic vibration control solution is discussed.

KEYWORDS

Viscoelastic material, above ground pipeline, vibration control, numerical simulation.

INTRODUCTION

Pipeline systems are commonly used to transport oil, natural gas, water, sewage and other materials. They are normally regarded as important lifeline structures. Ensuring the safety of these pipeline systems is crucial to the economy and environment. There are many reasons that may result in the damages to pipelines and these damages are often associated with pipeline vibrations. For example, vortex can lead to continuous vibrations of subsea pipeline and reduce its fatigue life (Kumar et al. 2008); vibrations induced by strong earthquakes may induce excessive stresses in the pipe wall and result in damage (Zeinoddini et al. 2012). Therefore, it is important to control pipeline vibrations to reduce the possibility of catastrophic damages.

Constrained viscoelastic layers have been widely used to reduce excessive vibrations of engineering structures due to its effectiveness and simplicity (e.g. Saidi et al. 2011; Borges et al. 2014). Normally a layer or multiple layers of viscoelastic materials (VEM) and a constraining layer (CL) are added to the original structure. The shear deformation of the VEM can obviously increase the damping of the original structure which in turn reduces its vibration. Extensive research efforts have been made to study the vibration characteristics of beam and plate structures with constrained damping layer. For the vibration and damping characteristics of cylindrical shells with constrained damping layer(s), the investigations are relatively less and the natural frequencies and damping of the constrained shell were generally derived based on the finite element method. For example, Chen and Huang (1999) presented a mathematical model for a cylindrical shell with partially constrained layer damping treatment. A thin shell theory in conjunction with the Donnell-Mushtari-Vlasov assumptions is employed to yield the model. Wang and Chen (2004) derived the equations of motion for the composite system based on a discrete layer theory. Many formulas were included in these studies, which impedes the application of these theories by researchers and especially engineers. A more readily applicable method, e.g. the numerical simulation method presented in this study, is deemed necessary.

This paper investigates the effectiveness of using constrained VEM layers to mitigate seismic induced vibrations of above ground pipelines. This idea originates from the recent work done by Borges et al. (2014), in which they proposed and investigated a concept aimed at suppressing vibrations in steel catenary risers by the use of viscoelastic sandwich layers. A series of experimental studies were carried out to find out the frequencies and damping of different vibration modes of the riser equipped with different scenarios of VEM. Instead of performing experimental studies, numerical simulations are carried out in the present study to investigate the effectiveness of using viscoelastic materials as the seismic vibration control solution to above ground pipelines by using the commercial software package ANSYS. The numerical model of the viscoelastic material is

calibrated based on the experimental data obtained from testing a 1.6m long tubular sandwich structure (Borges et al. 2014). The calibrated model is then applied to the above ground pipeline system. The effectiveness of using constrained VEM as the seismic vibration control solution is investigated.

NUMERICAL MODEL CALIBRATION

To carry out the numerical analysis, a reliable finite element model should be firstly developed. The experimental study carried out by Borges et al. (2014) is used as the reference to calibrate the finite element model. The numerical results are compared with the experimental data. For completeness, the experimental studies are briefly introduced in this section, more detailed information can be found in Borges et al. (2014).

Tested Original and Sandwich Tubes

Borges et al. (2014) carried out a series of experimental studies to identify the modal parameters (vibration frequencies and damping) of the original structure and structures assembled with different VEMs and CLs. The original structure consists of a brass beam with tubular cross section that is cantilevered at one end and free at the other. The length of the original structure is 1.6 m. To increase the damping of the original structure, viscoelastic layers and its associated brass constraining layers are assembled. The VEM used is the self-adhesive double face tape under code VHB4955, manufactured by 3M®. The viscoelastic and constraining layers are designed to be free at the both ends. Figure 1 shows the cross section of the sandwich beam and Table 1 presents the geometric properties of the tube layers.

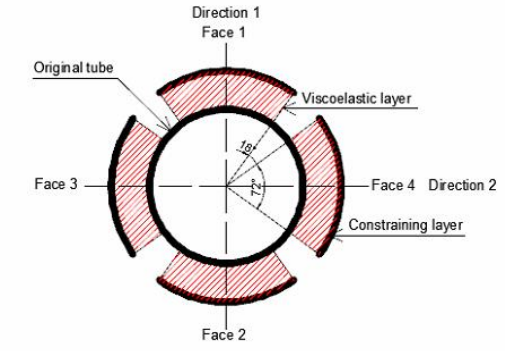

Figure 1 Tubular cross section of the sandwich beam structure (not to scale)

Table 1 Geometric properties of the tube layers (Borges et al. (2014))

Layer (material)	Length (mm)	External radius (mm)	Thickness (mm)
Internal tube (Brass)	1600	9.46	1.06
Viscoelastic material (VHB4955)	1600	11.86	2.4
Constraining (Brass)	1600	12.66	0.8

For the brass original tube and CLs, the Young's modulus is E_t=121.8 GPa and the density is ρ_t=8770 kg/m^3. For a linear, homogeneous and isotropic VEM, the complex shear modulus can be expressed in the frequency domain as

$$G^*(\omega)=G(\omega)[1+i\beta(\omega)] \quad (1)$$

where $G(\omega)$ is the storage modulus, $\beta(\omega)$ is the dissipation loss factor and ω is the circular frequency in rad/s. For the VEM used in the present study, the following parameters are identified (Stutz et al. 2009): Young's modulus E=6.88 MPa, density ρ=795 kg/m^3, Poisson's ratio υ=0.49 and dissipation loss factor β=0.75. The shear modulus is thus $G=E/[2(1+\upsilon)]$=2.31 MPa.

It can be seen from Figure 1 that the original tube was not fully covered by the VEMs and CLs, a gap was designed between different faces of cover layers. The angle of the gap was not mentioned by Borges et al. (2014). Based on the provided figure (Figure 8 in Borges et al. (2014)), the angle is estimated to be 18º and used in the present study, the angle of each constraining layer is thus 72º as shown in Figure 1.

Finite Element Modelling

The original tube, VEMs and CLs are all modelled with solid element SOLID186 in ANSYS, this element supports viscoelasticity. In the numerical model, the circumference of the original tube is divided into 40

elements. In the radial direction, the original tube and CLs are modelled by one element respectively while the VEMs are divided into two. In the longitudinal direction, the element size is 16 mm. The VEMs are rigidly connected to the original tube and CLs, namely the VEMs share nodes with the original tube and CLs. The cross section of the original tube is relatively small compared to its length, plotting the whole FE model will make the figure not clear, Figure 2 shows part of the FE model of the original tube with faces 1 and 2 (see Figure 1) constrained by VEMs and CLs.

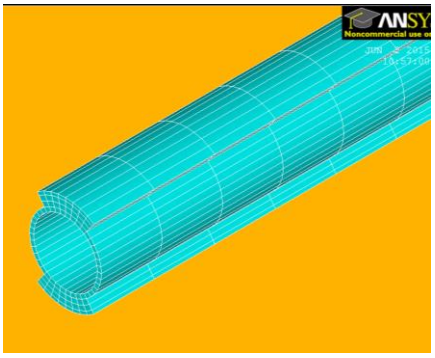

Figure 2 FE model of the original tube with faces 1 and 2 constrained with VEMs and CLs

The constraining layers are assumed to be linear elastic, while the VEM is assumed to be hyperelastic (Saidi et al. 2011). The damping is modelled in ANSYS for each material as a constant stiffness multiplier (DAMP command in ANSYS), which can be calculated from (Saidi et al. 2011):

$$\alpha_2 = \xi/(\pi f) \tag{2}$$

where α_2 is the stiffness multiplier, f is the fundamental vibration frequency of the structure, which can be obtained by carrying out an eigenvalue analysis, ξ is the damping ratio of the material. For the viscoelastic material, ξ is related to the dissipation loss factor β and can be estimated as $\xi=\beta/2$ (Nashif 1985). For the original tube, the damping ratio is 0.05% based on the test results.

Numerical and Experimental Results

Three different types of structures were tested by Borges et al. (2014), i.e. the original tube, the tube with faces 1 and 2 constrained with VEMs and CLs, and the tube with all faces constrained. The modal parameters in directions 1 and 2 (Figure 1) were experimentally identified. All these three different cases are numerically simulated. Due to the limitation of the page length, only the results of the original tube and the tube with faces 1 and 2 constrained are compared with the experimental data.

There are many methods available to identify the modal parameters once we have the free vibration data of the system. In the present study, the wavelet transform method proposed by Ruzzene et al. (1997) is adopted. This method is drawn upon the unique characteristics of Morlet wavelets, and the modal parameters are identified from the modulus and phase angle of the wavelet transform of the free vibration data. To identify the modal parameters in these two different directions, a 5 mm initial displacement is introduced in directions 1 and 2 respectively at the free end of the system and then released suddenly to simulate a free vibration test. The free vibration responses are then used as input to identify the modal parameters.

Tables 2 to 3 tabulate the identified modal parameters of the first two modes at directions 1 and 2 of different structures based on the numerical results and the corresponding values obtained from the tests. The differences between the numerical and experimental results, which are calculated from $(R_N-R_E)/R_E$, are also tabulated, where R_N and R_E represent the numerical and experimental results respectively. It is noted that the sampling frequency of the numerical results is 500 Hz in the present study. As shown in Tables 2 and 3, the modal parameters identified from the numerical results coincide well with those from the experimental tests. Large differences occur at the damping ratio of the original tube. This is because, as can be seen from Table 2 that the absolute value of the experimental results are quite small (0.03% to 0.05%), a slight deviation from the experimental results can lead to a large difference. The numerical simulation adopted in the present paper is therefore believed able to realistically model the VEM and the sandwich structure. It also can be seen from the tables that the constrained VEM can significantly increase the damping ratio of the structure. It thus has the potential to reduce the vibration of the original structure.

It should be noted that the tested original tube presented some imperfections in the test (Borges et al. 2014). The natural frequencies in the two different directions obtained from the tested data are slightly different as shown in

Table 2. In the numerical simulation, these imperfections are not considered, and the corresponding values in these two different directions are therefore the same for the original tube.

Table 2 Comparison of the modal parameters identified from the numerical results and the corresponding experimental results (the original tube)

Mode No	Numerical results				Experimental results				Difference (%)			
	Frequency (Hz)		Damping ratio (%)		Frequency (Hz)		Damping ratio (%)		Frequency		Damping ratio	
	Dir. 1	Dir. 2	Dir. 1	Dir. 2	Dir. 1	Dir. 2	Dir. 1	Dir. 2	Dir. 1	Dir. 2	Dir. 1	Dir. 2
1	5.15	5.15	0.07	0.07	5.17	5.12	0.05	0.05	-0.39	0.59	40	40
2	31.82	31.82	0.06	0.06	32.11	31.89	0.04	0.03	-0.90	-0.22	50	100

Table 3 Comparison of the modal parameters identified from the numerical results and the corresponding experimental results (the tube with faces 1 and 2 constrained)

Mode No	Numerical results				Experimental results				Difference (%)			
	Frequency (Hz)		Damping ratio (%)		Frequency (Hz)		Damping ratio (%)		Frequency		Damping ratio	
	Dir. 1	Dir. 2	Dir. 1	Dir. 2	Dir. 1	Dir. 2	Dir. 1	Dir. 2	Dir. 1	Dir. 2	Dir. 1	Dir. 2
1	5.11	4.51	5.03	0.24	4.85	4.23	5.59	0.25	5.36	6.62	-10.02	-4.00
2	32.98	28.30	6.57	0.41	30.80	26.40	7.21	0.33	7.08	7.20	-8.88	24.24

ABOVE GROUND PIPELINES

Pipeline Details

Figure 3 shows a typical above ground pipeline supported on discrete supports at equal intervals. The pipeline is made of steel and the length of each span is 16 m. The outer diameter of the pipe cross section is 0.35 m and the thickness is 3 mm. The pipeline may undergo violent vibrations under severe earthquakes. To mitigate these adverse vibrations, VEM layers and CLs are proposed to be assembled on the surface of the original pipeline. In a real earthquake, three dimensional ground excitations are inevitable. To demonstrate the effectiveness of the proposed method, only the transverse earthquake loading is considered in the present study. The VEMs and CLs are only assembled in the transverse direction (x direction as shown in Figure 4) of the pipe.

Figure 3 A typical above ground pipeline

Seismic Ground Motion

The pipeline is located on a flat-lying soil site as shown in Figure 4. One single layer of soil rests on the base rock. The parameters of the soil layer and base rock are included in the figure, where ρ, G, ξ, υ and h represent the density, shear modulus, damping ratio, Poisson's ratio and thickness respectively. The lower cases s and b represent the soil layer and base rock. In the present study, the base rock motion is assumed to consist of out-of-plane SH wave and it is represented by a filtered Tajimi-Kanai power spectral density function as (Tajimi 1960)

$$S_g(\omega) = \frac{\omega^4}{(\omega_f^2 - \omega^2)^2 + (2\omega_f \omega \xi_f)^2} \frac{1 + 4\xi_g^2 \omega_g^2 \omega^2}{(\omega_g^2 - \omega^2)^2 + 4\xi_g^2 \omega_g^2 \omega^2} \Gamma \tag{3}$$

where ω_g and ξ_g are the central frequency and damping ratio of the Tajimi-Kanai power spectral density function, ω_f and ξ_f are the corresponding central frequency and damping ratio of the high pass filter function. Γ is a scaling factor depending on the ground motion intensity. The parameters for the transverse motion are assumed as $\omega_g = 10\pi$ rad/s, $\xi_g = 0.6$, $\omega_f = 0.5\pi$, $\xi_f = 0.6$ and $\Gamma = 0.0212$ m^2/s^3. These parameters correspond

to a ground motion time history with duration T=16 s and PGA of 0.5g based on the standard random vibration method (Der Kiureghian 1980).

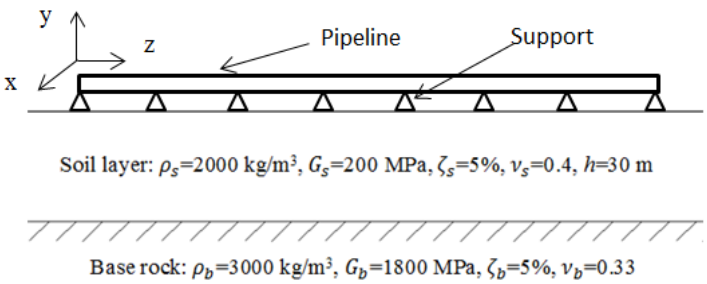

Figure 4 Numerical model of an above ground pipeline and underneath site conditions (not to scale)

The base rock motion can be further filtered and amplified by the soil layer. The transverse earthquake loading on the ground surface can be simulated based on the combined spectral representation method and one-dimensional wave propagation method (Bi and Hao 2012). Figure 5 shows the simulated transverse acceleration time history. It is worth to note that in the simulation, the sampling frequency and the upper cut-off frequency are set to be 100 and 25 Hz respectively. Figure 6 shows the comparison of the simulated power spectral density (PSD) with the theoretical value which is derived based on the one-dimensional wave propagation theory (Wolf 1985). Good agreements are observed.

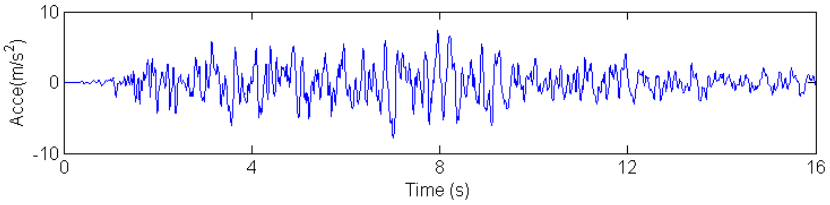

Figure 5 Simulated transverse acceleration time history

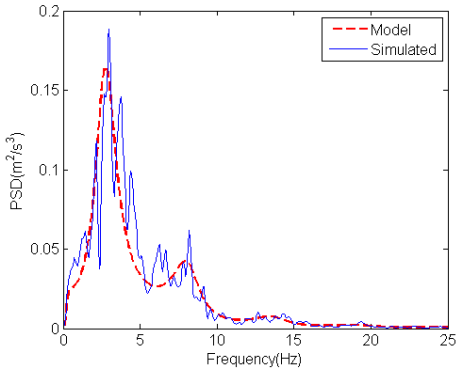

Figure 6 Comparison of the PSDs of the simulated ground motion with the theoretical model

Numerical Model

The viscoelastic material VHB4955 manufactured by 3M® calibrated in Section 2 is used again to increase the damping of the original pipeline. The sandwich pipeline is modelled the same way as the sandwich tube in Section 2. The original pipe and the CLs are made of steel and the Young's modulus, density and Poisson's ratio are 210 GPa, 7800 kg/m^3 and 0.3 respectively. Normally the pipe is not fully fixed to the supports, the transverse restraint provided by the support can be considered by a spring. The stiffness of the spring normally varies from 7.5x10^5 N/m to 6x10^6 N/m (Anderson and Johnston 1975). In the present study, the transverse restraints provided by the supports are modelled by the COMBIN14 elements, and its stiffness is 1.1644x10^6 N/m (Soliman and Datta 1996). In the vertical direction, the pipeline is assumed to be simply supported by the supports. The damping ratio of the original pipeline is assumed to be 1.2% in the present study.

Since it is impossible to model the whole length of a pipeline system, taking one span of the entire pipeline out for analysis is more practical. To simulate the restraining effects from adjacent spans to the single-span model,

rotational springs are added at the both ends of the analysed span (Bao et al. 2013), and they are modelled by COMBIN14 elements again. The rotational spring stiffness is determined by performing a numerical convergence analysis and a value of 1.465×10^5 Nm/rad is determined. Figure 7 shows part of the single-span model, in which part of the span in assembled with VEMs and CLs. In the subsequent analysis, only the single-span model with the rotational spring at the both supports is analysed. This substantially reduces the computational time for the analysis.

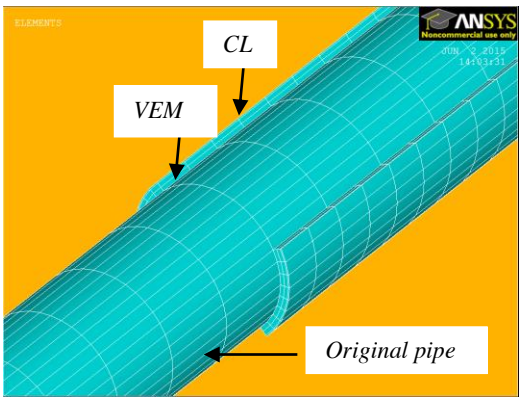

Figure 7 Finite element model of a single-span pipeline with part of the span assembled with VEMs and CLs

NUMERICAL RESULTS

This section carries out numerical simulations on the effectiveness of using constrained VEMs to mitigate the seismic induced vibrations of above ground pipelines. For comparison, the corresponding results from the original pipeline are also presented.

The acceleration time history shown in Figure 5 is used as input in the transverse direction of the pipeline. The duration of the earthquake loading is 16 sec. In the numerical simulation, a 20 sec response is calculated. In the first 16 sec, the pipeline system is subjected to the transverse earthquake loading (forced vibration), while it vibrates freely in the last 4 sec. The acceleration response in the free vibration phase is used to identify the modal parameters, i.e., natural frequency and damping ratio of the system, based on the wavelet transform method proposed by Ruzzene et al. (1997) with a sampling frequency of 100 Hz. Since the transverse input is considered in the present study, only the vibration frequency and damping ratio corresponds to the first transverse vibration mode are presented and discussed. For the original pipeline, the fundamental vibration mode is in the transverse direction with a frequency of 3.8369 Hz based on an eigenvalue analysis. By using the free vibration result, the identified frequency and damping ratio is 3.8556 Hz and 1.25% respectively, which are close to the vibration frequency obtained from the eigenvalue analysis and the assumed damping ratio of 1.2%. All the modal parameters presented in this section are the identified values based on the single-span pipeline model.

Influence of Constraining Arrangement Scenarios

Borges et al. (2014) experimentally identified the vibration frequencies and damping of the original riser with the viscoelastic sandwich layers sequentially assembled in segments along the original structure. This segmented arrangement (Figure 8(a)) as suggested by Borges et al. (2014) is firstly investigated in the study. The length for each segment is 2 m and the spacing between adjacent segments is 1 m. 1, 3 and 5 constraining segments are considered as shown in Figure 8(a). Another two arrangement scenarios, namely the compact configuration shown in Figure 8(b) and the monolithic configuration shown in Figure 8(c), are also investigated. In the compact configuration, the constraining segments concentrate at the centre of the span and there is no gap between each segment. For the monolithic configuration, all the segments are rigidly connected together to form an integral constrain. In all these cases, the thickness of the VEM layers is 20 mm and the thickness of the CLs is 3 mm.

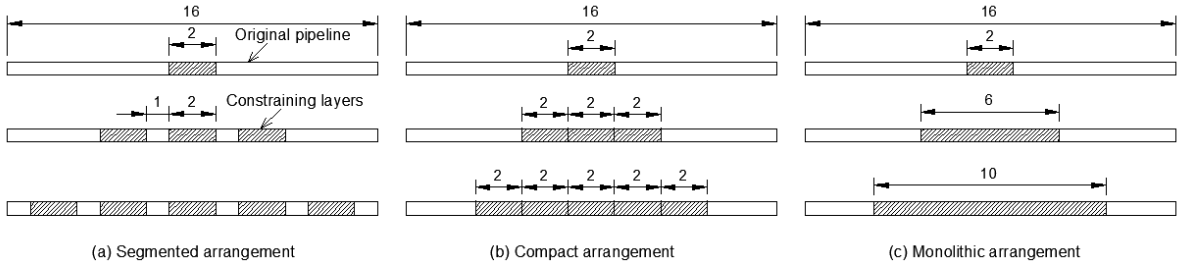

Figure 8 Constraining arrangement scenarios: (a) segmented, (b) compact and (c) monolithic configurations (unit: meter)

Table 4 tabulates the identified fundamental transverse vibration frequencies and the corresponding damping ratios of different constraining arrangement cases. The results obtained from the original pipeline (constraining length L=0 m) are also shown. It can be seen from the table that for the segmented and compact arrangements, increasing the number of constraining segments leads to the monotonous decreasing of vibration frequency of the system. For the monolithic arrangement, the vibration frequency decreases with the increasing of the constraining length if the constraining length is less than 6 m. When the constraining length reaches 10 m, the vibration frequency of the system is, however, larger than the pipeline with the constraining length of 6 m. This is because the vibration frequency is determined by the mass and stiffness of the system. For the segmented and compact arrangements, the segments contribute relatively small to the stiffness of the system because of the short length of the segments (2 m in the present study). Increasing the segment numbers, however, obviously increases the mass of the system, which in turn results in the smaller vibration frequency. For the monolithic arrangement with long enough VEMs and CLs, the constraining layers will evidently increase the stiffness of the system as well, besides their contributions to the mass. When the contribution to the stiffness is larger than that of the mass, larger vibration frequency will be obtained. It also can be seen from the table that the compact arrangement leads to smaller vibration frequency of the system compared to the segmented configuration. This is because the segments contribute more to the total mass of the system when they are more concentrated to the centre of the span.

The table also shows that the segmented and compact arrangements only slightly increase the damping ratio of the system. For the original pipeline, the identified damping ratio is 1.25%. When 2, 6 and 10 m constraining layers are assembled, the damping ratios are 1.43%, 1.67% and 1.70% respectively for the segmented arrangement. The corresponding values for the compact arrangement are 1.43%, 1.69% and 1.81%. On the other hand, the increasing in damping of the system is quite obvious if the constraining layers are assembled monolithically when the length of the constraining layers is not too short. For example, the damping ratios reach 3.53% and 4.78% when the constraining lengths are 6 and 10 m respectively. This is because the high damping capacity of structure with constrained damping layer is mostly due to the shear deformation of the VEM (Wang and Cheng 2004). With the same length of constraining layers, the VEMs and CLs undergo larger shear deformation during vibration when monolithic arrangement is considered and thus larger damping ratio is expected.

Table 4 Identified frequencies and damping ratios of different constraining scenarios

Constraining Length	Frequency (Hz)			Damping ratio (%)		
	Segmented	Compact	Monolithic	Segmented	Compact	Monolithic
0	3.8556	3.8556	3.8556	1.25	1.25	1.25
2	3.5675	3.5675	3.5675	1.43	1.43	1.43
6	3.2513	3.1927	3.3387	1.67	1.69	3.53
10	3.1749	3.0120	3.4105	1.70	1.81	4.78

The constraining layers can significantly influence the seismic responses of the system. Figure 9 shows the transverse displacement time histories at the middle span of the pipelines with different scenarios of constrains. Only the forced vibration responses are plotted in the paper. The results are compared with that obtained from the original structure. As shown, when segmented or compact arrangement is adopted, the suppressing of vibrations is not obvious because the damping ratios only increase slightly in these cases as shown in Table 4. Moreover, it can be seen that more constraining segments do not necessarily result in more effective vibration reduction. This is most evident for the case where the pipeline is compactly assembled with five segments

(L=10 m). This system vibrates even more violently than the original pipeline. This is because the addition of the segments obviously changes the vibration frequency of the system while it does not increase the damping evidently. As can be seen from Table 4, the vibration frequencies for the original pipeline and the pipeline with five compact segments are 3.8556 and 3.0120 Hz respectively. Moreover, Figure 6 shows that the energy of the earthquake loading mainly concentrates around 2.734 Hz due to the local site amplification effect. This frequency is close to the vibration frequency of the compact scenario (3.0120 Hz), which means that when the pipeline is compactly assembled with five segments, resonance can occur and larger seismic response is expected. When monolithic arrangement is adopted, the reduction of vibration is significant as shown in Figure 9(c) due to the obvious increment of damping. Of course, the decreased vibration frequency makes the system vibrates closer to the resonant frequency of local soil site, however, this effect is compensated by the increased damping ratio of the system. The results suggest that monolithic arrangement is more effective than the segmented and compact arrangements in the seismic vibration control of above ground pipeline considered in this study.

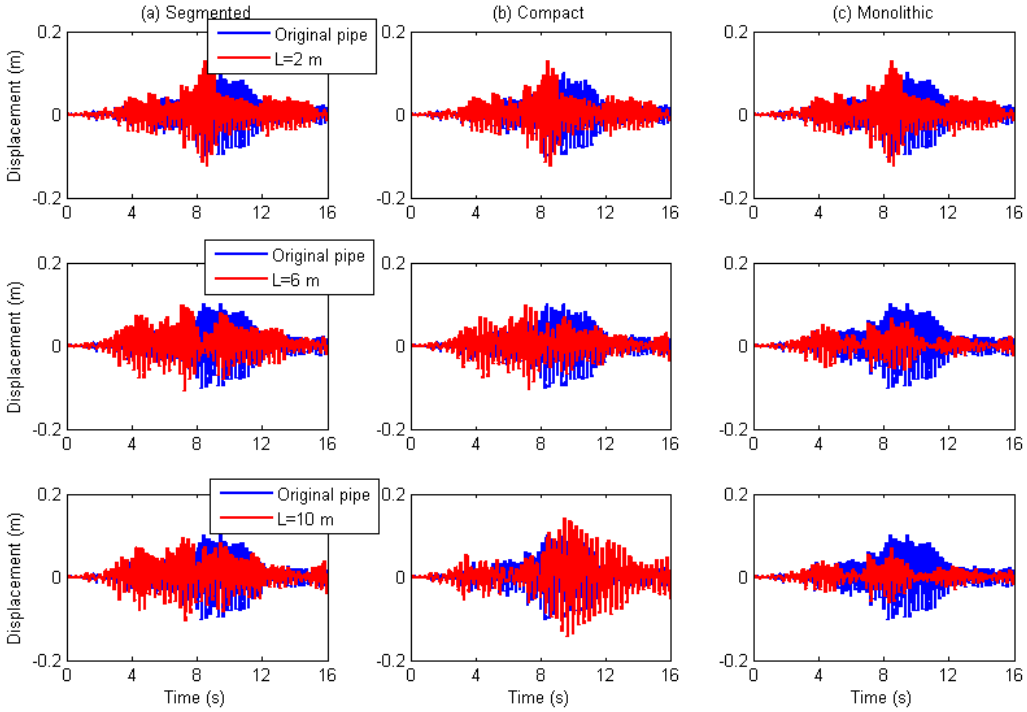

Figure 9 Influence of constraining arrangements on the seismic responses of the system: (a) segmented, (b) compact and (c) monolithic configurations

Influence of Different Earthquake Loadings

In the previous section, the artificially simulated earthquake loading is used as input in the numerical simulation. To further examine the influence of ground motion frequency content on the effectiveness of the proposed method, the seismic responses of the original and constrained pipelines subjected to two natural earthquake loadings obtained from the database of Pacific Earthquake Engineering Research Centre are also calculated and compared. The first earthquake loading is the record from the 1994 Northridge earthquake. This earthquake loading is characterized by the long-period pulse-like waveforms, and it is normally classified as near-field ground motion. The second record is from the 1971 San Fernando earthquake, which exhibits fewer long-period characteristics and it is used to represent far-field earthquake. Table 5 summarises these two earthquake components and Figure 10 shows the accelerograms of the two ground motions. Figure 11 plots the PSDs of these two earthquake loadings. It can be seen that the energies of the Northridge earthquake loading mainly concentrate in the frequency band less than 2 Hz and for the San Fernando earthquake, they are mainly in the frequency band less than 1 Hz. The dominant frequencies of these two earthquakes are far from the first vibration frequencies of the original and constrained pipelines, which are 3.8556 and 3.4105 Hz respectively as mentioned above. The changes in the seismic responses are thus mainly because of the change of the damping. Figure 12 shows the seismic responses of the original and constrained pipelines subjected to these two earthquake loadings. It is obvious that the proposed method is effective to suppress the vibrations induced by these two natural earthquake loadings.

Table 5 Two natural earthquake records

Earthquake	Date	Station	Component
Northridge	17/01/1994	Sylmar	NS
San Fernando	09/02/1971	2516 Via Tejon PV	NS

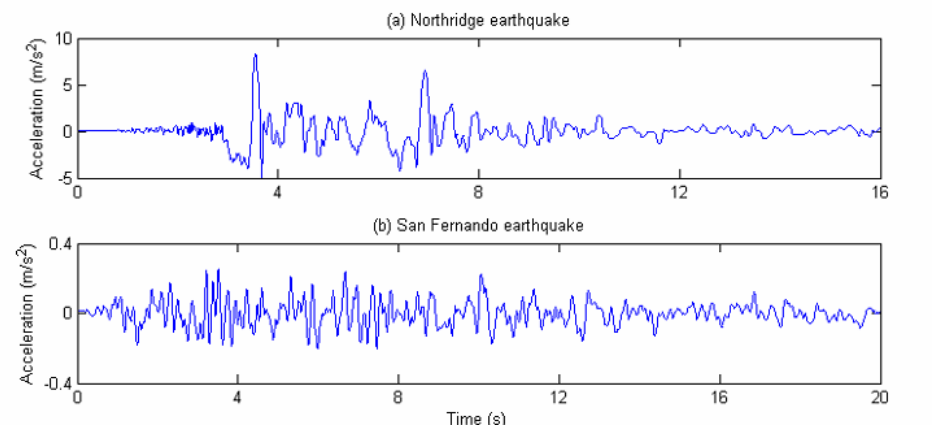

Figure 10 Accelerograms of the selected Northridge and San Fernando earthquake loadings

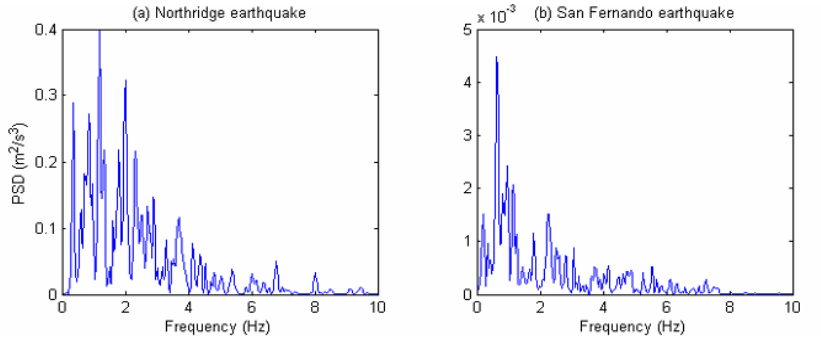

Figure 11 PSDs of the selected Northridge and San Fernando earthquake loadings

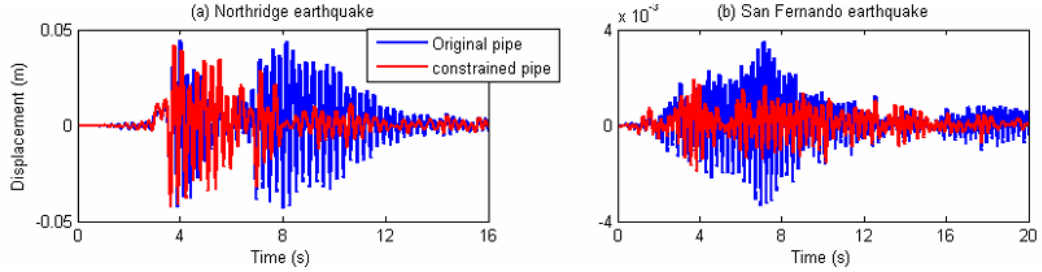

Figure 12 Seismic responses of the original and constrained pipelines subjected to (a) Northridge and (b) San Fernando earthquakes

CONCLUSIONS

This paper carries out numerical simulations on the effectiveness of using viscoelastic materials to mitigate seismic induced vibrations of above ground pipelines. The modelling of the viscoelastic material is firstly calibrated based on the experimental data obtained from testing a 1.6 m long tubular sandwich structure. The calibrated model is then applied to the above ground pipeline system. Man-made, far-field and near- field earthquake ground motions are considered as input in the numerical analyses. Numerical results show that it is effective to mitigate the seismic induced vibrations of above ground pipelines by assembling the VEMs and CLs

to the original pipeline structure. It also finds that monolithic arrangement is more effective than segmented and compact arrangements in increasing the damping of the original pipeline system and suppressing its vibration.

ACKNOWLEDGMENTS

The first author would like to acknowledge the support from Australian Research Council Discovery Early Career Researcher Award DE150100195 for carrying out this research.

REFERENCES

Anderson, J.C. and Johnston, S.B. (1975). "Seismic behavior of above-ground oil pipeline". *Earthquake Engineering and Structural Dynamics*, 3, 319-336.

Bao, C., Hao, H. and Li, Z.X. (2013). "Integrated ARMA model method for damage detection of subsea pipeline system". *Engineering Structures*, 48, 176-192.

Bi, K. and Hao, H. (2012). "Modelling and simulation of spatially varying earthquake ground motions at sites with varying conditions". *Probabilistic Engineering Mechanics*, 29, 92-104.

Borges, F.C.L., Riotman, N., Magluta, C., Castello, D.A. and Franciss, R. (2014). "A concept to reduce vibrations in steel catenary risers by the use of viscoelastic materials". *Ocean Engineering*, 77, 1-11.

Chen, L.H. and Huang, S.C. (1999). "Vibrations of a cylindrical shell with partially constrained layer damping (CLD) treatment". *International Journal of Mechanical Sciences*, 41, 1485-1498.

Der Kiureghian, A. (1980). "Structural response to stationary excitation". *Journal of Engineering Mechanics Division* 1980; 106(6): 1195-213.

Kumar, R.A., Sohn, C.H. and Gowda, B.H.L. (2008). "Passive control of vortex-induced vibrations: an overview". *Recent Patents on Mechanical Engineering*, 1, 1-11.

Nashif, A.D. (1985). *Vibration damping*. John Wiley & Sons, New York, USA.

Ruzzene, M., Fasana, A., Garibald,i L. and Piombo, B. (1997). "Natural frequencies and dampings identification using wavelet transform: application to real data". *Mechanical Systems and Signal Processing*, 11(2), 207-218.

Saidi, I., Gad, E.F., Wilson, J.L. and Haritos, N. (2011). "Development of passive viscoelastic damper to attenuate excessive floor vibrations". *Engineering Structures*, 33, 3317-3328.

Soliman, H.O. and Datta, T.K (1996). "Response of overground pipelines to random ground motion". *Engineering Structures*, 18(7), 537-545.

Stutz, L.T., Magluta, C., Roitman, N., Silva, R.P. (2009). "Experimental and numerical analysis of a sandwich beam with viscoelastic layer". *Proceedings of the 20th international congress of mechanical engineering*, 15-20 November, Gramado, Brazil.

Tajimi, H. (1960). "A statistical method of determining the maximum response of a building structure during an earthquake". *Proceedings of 2nd World Conference on Earthquake Engineering*, Tokyo, Japan.

Wang, H.J. and Chen, L.W. (2004). "Finite element dynamic analysis of orthotropic cylindrical shells with a constrained damping layer". *Finite Elements in Analysis and Design*, 40, 737-755.

Wolf, J.P. (1985). *Dynamic soil-structure interaction*. Englewood Cliffs, New Jersey, USA.

Zeinoddini, M., Parke, G.A.R. and Sadrossadat, S.M. (2012). "Free-spanning submarine pipeline response to severe ground excitations: water-pipeline interactions". *Journal of Pipeline Systems Engineering and Practice ASCE*, 3(4), 135-149.